



# Transport coefficients in standard Kappa distributed plasmas

Mahmood J. Jwailes , Imad A. Barghouthi , and Qusay S. Atawnah

Department of physics, Al-Quds university, Jerusalem, Palestine.

**Correspondence:** Mahmood J. Jwailes (mahmood.jwailes@students.alquds.edu)

**Abstract.** This study presents a systematic derivation of transport coefficients—including electrical conductivity, thermoelectric, diffusion, and mobility coefficients—for a Lorentz plasma described by a standard Kappa distribution function. The analysis is implemented within the framework of the five-moment transport equations, in which the standard Kappa distribution is adopted as the zeroth-order function. Momentum and energy collision terms are then evaluated using the Boltzmann collision 5 integral for several types of collisions, including Coulomb collisions, hard-sphere interactions, and Maxwell molecules. These collision terms are incorporated into the momentum equation to construct expressions for the generalized Ohm's law and extended Fick's law, from which the transport coefficients are obtained. The influence of the kappa parameter on the collision terms and transport coefficients is examined in detail, revealing that low kappa values reduce the effective collision frequency and enhance transport coefficients in the standard Kappa distribution, in contrast to the behavior reported for the modified 10 Kappa distribution. Finally, in the asymptotic limit of large kappa values, the transport coefficients consistently recover their Maxwellian forms.

## 1 Introduction

Transport processes in plasma can be analyzed using transport equations, which provide a macroscopic description of the spatial and temporal evolution of the velocity moments of the particles velocity distribution function. These moments (e.g. 15 number density, drift velocity, temperature, pressure tensor, stress tensor, and heat flow vector) capture the collective behavior of plasma particles and interactions that determine their dynamics (Schunk, 1977; Schunk and Nagy, 2009; Bittencourt, 2004). The transport equations are based on linear relationships between the fluxes (e.g., particle flux, heat flux, and current density), the external forces and gradients (e.g., in density, temperature, and pressure) that drive those fluxes. The constants of proportionality in these linear relations are called transport coefficients—namely, the diffusion coefficient, electrical conductivity, mobility coefficient, thermoelectric coefficient, and thermal conductivity—which quantify how particles and energy 20 move through a plasma under the influence of gradients, external forces, and applied electromagnetic forces. Each coefficient characterizes a different aspect of transport, that is, the diffusion coefficient measures the flux of particles driven by spatial variations in density, providing insight into how species spread within the plasma. The mobility coefficient describes how charged particles drift in response to an applied electric field, and it is directly related to the electrical conductivity, which connects the 25 current density to the electric field. The thermoelectric coefficient links electric fields to temperature gradients and characterizes the generation of electric voltages and currents in non-uniform thermal environments. Finally, the thermal conductivity



determines the heat flux produced by temperature gradients and governs the rate of thermal energy transport within the plasma (Du, 2013; Wang and Du, 2017; Ebne Abbasi et al., 2017; Ebne Abbasi and Esfandyari-Kalejahi, 2019; Guo and Du, 2019; Husidic et al., 2021).

30 For plasmas near thermal equilibrium, the Maxwellian distribution is commonly used to evaluate transport coefficients. However, space and astrophysical plasmas often contain nonthermal particle populations that cause particle velocity distributions to deviate from the Maxwellian form. In these nonthermal environments, such distributions are well fitted by the Kappa velocity distribution functions (Marsch, 2006). Kappa distributions are considered powerful class of non-Maxwellian distributions, characterized by a power-law tail that captures the presence of suprathermal particles, features that the Maxwellian distribution  
35 fails to describe.

Consequently, several studies have extensively investigated transport coefficients in nonequilibrium plasmas using the Kappa velocity distribution functions. In particular, studies such as Du (2013); Wang and Du (2017); Ebne Abbasi et al. (2017); Ebne Abbasi and Esfandyari-Kalejahi (2019); Guo and Du (2019); Jwailes et al. (2025) derived diffusion, mobility, electrical conductivity, thermoelectric coefficients, and thermal conductivity based on modified Kappa distributions, which assume a  $\kappa$ -  
40 independent effective temperature and therefore produce a stronger low-energy core and enhanced suprathermal tails relative to a Maxwellian. Here, the kappa parameter  $\kappa$ , controls the population of high-energy suprathermal particles. However, this modified form differs fundamentally from the standard (Olbertian) Kappa distribution, introduced by Olbert (1968) and Vasyliunas (1968), in which the effective temperature is  $\kappa$ -dependent, leading to weaker core and more pronounced high-energy tails. This  
45 motivated Husidic et al. (2021) to evaluate the same transport coefficients for the standard Kappa distribution, demonstrating that distinctions between the two forms are crucial because the choice of distribution impacts the resulting transport coefficients and their physical interpretation.

All of the reviewed studies used simplified collision models rather than the full Boltzmann collision integral. The simplest models appear in Wang and Du (2017), Ebne Abbasi and Esfandyari-Kalejahi (2019), and Husidic et al. (2021) which used Krook-type or BGK operators, offering computational simplicity but limited accuracy. More physically based models—such as  
50 those proposed by Du (2013) and Guo and Du (2019)—used macroscopic transport equations derived from idealized relaxation assumptions. The most advanced work, presented by Ebne Abbasi et al. (2017), used the Fokker-Planck equation to model Coulomb collisions. While this captures cumulative small-angle scattering and better represents long-range Coulomb forces, it remains an approximation of the Boltzmann collision integral. Thus, all reviewed works share the same limitation: reliance  
55 on simplified collision models. To overcome this limitation, Jwailes et al. (2025) recently introduced a comprehensive re-evaluation of the transport coefficients based on the modified Kappa distribution, using the five-moment approximation of the transport equations with the Boltzmann collision integral as the collision model. In this approach, a new transport theory is developed by deriving the five-moment approximation and the corresponding collision terms for various types of collisions for the modified Kappa distribution. The five-moment momentum equation is then linked to the generalized Ohm's law and the extended Fick's law, from which the transport coefficients are determined.

60 This study is inspired by the work of Husidic et al. (2021) and follows the same methodology and steps introduced by Jwailes et al. (2025). As in Husidic et al. (2021), we focus on evaluating the transport coefficients for the standard Kappa distribution,



but we adopt the methodology used in Jwailes et al. (2025), particularly in the formulation of the transport equations, the evaluation of the collision integrals, and the derivation of the transport coefficients. However, in contrast to Husidic et al. (2021), we use the Boltzmann collision integral as our collision model rather than the Krook-type collision model. This substitution  
65 is essential for obtaining results that more accurately capture the velocity-dependent interaction dynamics inherent to Kappa-distributed plasmas.

This paper is structured as follows: Section 2 provides a brief review of the Kappa distribution family, introducing the mathematical formulations and the physical interpretation of two different types of suprothermal tail distributions: the standard Kappa and the modified Kappa distribution functions. It also explains how their behaviors differ from that of the Maxwellian  
70 distribution. Section 3 presents the theoretical framework of this paper, in which we derive the five-moment approximation and the corresponding collision terms for the standard Kappa velocity distribution function, considering arbitrary drift-velocity and temperature differences between the interacting plasma species. This includes three types of collisions: Coulomb collisions, hard-sphere interactions, and Maxwell-molecule collisions. The section concludes with the derivation of the transport coefficients using the five-moment approximation and the derived collision terms. Section 4 discusses the derived results presented  
75 in Section 3 for the standard Kappa distribution and compares them with the corresponding results for both the modified Kappa distribution and the Maxwellian distribution. Three aspects are considered in the comparison: (i) the effective collision frequency and thermalisation rate; (ii) the behavior of the collision terms in the case of Coulomb collisions, with a focus on how collisions affect both the momentum and the energy of the interacting particles; and (iii) the transport coefficients and their dependence on the kappa parameter. The derived formulas are also compared with results from previous studies, highlighting  
80 their dependence on the kappa parameter. Finally, Section 5 presents the conclusions.

## 2 Distributions with suprothermal tails

Kappa distributions constitute a broad class of non-Maxwellian velocity distribution functions that effectively describe suprothermal particle populations in space and astrophysical plasmas. Unlike the Maxwellian distribution, they introduce a power-law tail that decays more slowly than the exponential tail of the Maxwellian. This tail is controlled by the kappa parameter  $\kappa$ ,  
85 which determines the strength of the high-energy tail: larger  $\kappa$  values approach the Maxwellian limit, while smaller values emphasize suprothermal populations. With typical  $\kappa$  values ranging between 2 and 6, Kappa distributions have been observed across diverse plasma environments, including the solar wind, Earth's magnetosheath, and Jupiter's magnetosphere, supported by direct measurements from satellite missions such as Ulysses, Cluster, and Voyager 2 (see (Vasyliunas, 1968; Pierrard et al., 2001; Maksimovic et al., 1997; Qureshi et al., 2003; Formisano et al., 1973; Collier and Hamilton, 1995) for details on these  
90 missions and their observations of the Kappa distributions). Among the various formulations proposed in the literature, two main types are commonly used: the standard Kappa distribution and the modified Kappa distribution. While both distributions share the general objective of characterizing plasmas with high-energy tails, they differ in their mathematical structure, parameter definitions, and physical interpretations.



95 The concept of the Kappa distribution was first proposed by Olbert (1968) to explain the presence of high-energy particles  
 observed in the solar wind and magnetospheric plasmas, and was subsequently formalized by Vasyliunas (1968), who provided  
 a more rigorous mathematical formulation. This early version is commonly referred to as the Olbertian or standard Kappa  
 distribution (SK). In velocity space, the drifting standard Kappa distribution is given by, (Lazar and Fichtner, 2021),

$$100 f_s^{\text{SK}}(\mathbf{r}, \mathbf{c}_s, t) = \frac{n_s \xi(\kappa_s)}{\pi^{3/2} w_s^3} \left(1 + \frac{c_s^2}{\kappa_s w_s^2}\right)^{-\kappa_s - 1}, \quad (1)$$

where  $n_s$  denotes the number density and  $w_s$  is the thermal velocity of species  $s$ , defined as

$$100 w_s = \sqrt{\frac{2k_B T_s}{m_s}}, \quad (2)$$

with  $m_s$  and  $T_s$  being the particle mass and the absolute temperature, respectively, and  $k_B$  the Boltzmann constant. The random velocity  $\mathbf{c}_s$  is defined in terms of the position  $\mathbf{r}$ , velocity  $\mathbf{v}_s$ , and the drift velocity  $\mathbf{u}_s(\mathbf{r}, t)$  of the species  $s$ ,

$$105 \mathbf{c}_s(\mathbf{r}, \mathbf{v}_s, t) = \mathbf{v}_s - \mathbf{u}_s, \quad (3)$$

The normalization function  $\xi(\kappa_s)$ , which depends on the kappa parameter  $\kappa_s$ , is given by

$$110 \xi(\kappa_s) = \kappa_s^{-3/2} \frac{\Gamma(\kappa_s + 1)}{\Gamma(\kappa_s - 1/2)}. \quad (4)$$

The parameter  $\kappa_s$  determines the slope of the power-law tails. Within this framework, the effective temperature  $T_\kappa$ , obtained  
 via the second velocity moment, depends on the kappa parameter  $\kappa_s$  and is written as

$$115 T_\kappa = \frac{\kappa_s}{\kappa_s - 3/2} \frac{m_s w_s^2}{2k_B} = \frac{\kappa_s}{\kappa_s - 3/2} T_s. \quad (5)$$

As  $\kappa_s$  increases, the effective temperature decreases until it reaches the Maxwellian temperature  $T_s$ . This dependence implies  
 110 that the enhanced presence of suprathermal particles contributes additional energy to the system, effectively heating the plasma.  
 Moreover, the expression for the effective temperature in equation 5 imposes a condition on the kappa parameter, namely  
 $\kappa_s > 3/2$ ; below this value the effective temperature diverges and is therefore undefined (Pierrard and Lazar, 2010).

Decades later, inspired by the principles of non-extensive statistical mechanics introduced by Tsallis (2012), Livadiotis  
 (2017) developed a new theoretical perspective reformulated the Kappa distribution into what is now known as the modified  
 115 Kappa distribution (MK). In velocity space, the modified Kappa distribution is given by, (Livadiotis, 2018; Davis et al., 2023),

$$f_s^{\text{MK}}(\mathbf{r}, \mathbf{c}_s, t) = \frac{n_s \eta(\kappa_s)}{\pi^{3/2} w_s^3} \left(1 + \frac{c_s^2}{\kappa_{0s} w_s^2}\right)^{-\kappa_s - 1}, \quad (6)$$

where  $w_s$  is defined as in equation 2. The normalization function in this case takes the form

$$120 \eta(\kappa_s) = \kappa_{0s}^{-3/2} \frac{\Gamma(\kappa_s + 1)}{\Gamma(\kappa_s - 1/2)}, \quad \kappa_{0s} = \kappa_s - \frac{3}{2}. \quad (7)$$

Here,  $\kappa_{0s}$  represents the invariant Kappa index, while  $\kappa_s$  is the shape parameter that governs the slope of the suprathermal  
 tails. As before, the condition  $\kappa_s > 3/2$  must be satisfied to ensure that the modified Kappa distribution function in equation (7)



remains well defined. This modified version introduces a stronger thermodynamic basis by decoupling the effective temperature from the kappa parameter  $\kappa_s$ , making it a kappa independent quantity, as given by

$$T_\kappa = \frac{\kappa_{0_s}}{\kappa_s - 3/2} \frac{m_s w_s^2}{2k_B} = T_s, \quad (8)$$

which is identical to the Maxwellian temperature and remains constant regardless of the value of  $\kappa_s$ . This ensures that variations 125 in the high-energy tails do not change the overall thermal energy content of the plasma. In this sense, the modified Kappa distribution maintains the same total thermal energy content as a Maxwellian plasma while redistributing the particles between the core and tail regions.

On the similarity side, both the standard and modified Kappa distributions are used to describe particle populations with suprathermal tails, since both distributions retain a power-law form and exhibit suprathermal tails that are higher than those of 130 the Maxwellian distribution. Moreover, both distributions reduce to the Maxwellian distribution in the limiting case where  $\kappa_s$  approaches infinity, (Pierrard and Lazar, 2010).

$$\lim_{\kappa_s \rightarrow \infty} f_s^{\text{SK}} = \lim_{\kappa_s \rightarrow \infty} f_s^{\text{MK}} = \frac{n_s}{\pi^{3/2} w_s^3} \exp\left(-\frac{c_s^2}{w_s^2}\right). \quad (9)$$

This behaviour is illustrated in Figure 1, where increasing  $\kappa_s$  causes both the standard and modified Kappa distributions to converge smoothly toward the Maxwellian distribution. Although the standard and modified Kappa distributions share this 135 common limiting behavior and exhibit similar qualitative features, they differ in their mathematical formulation and physical interpretation. The mathematical distinction between the two forms lies primarily in their parameterization and normalization. The standard distribution employs  $\kappa_s$  in the energy-dependent term, while the modified version replaces it with  $\kappa_s - 3/2$ . While this shift may appear minor, it significantly affects the scaling of the velocity distributions, resulting slightly flatter high-energy tails in the modified Kappa distribution compared to the standard Kappa distribution for the same  $\kappa_s$  value. Moreover, 140 in the standard Kappa distribution, the effective temperature of the particles depends on  $\kappa_s$ , making it much higher than the temperature in the Maxwellian case. However, for the modified Kappa distribution, the effective temperature is independent of  $\kappa_s$ , making it identical to the Maxwellian temperature.

These differences are reflected in how the particle's velocity is distributed. To illustrate how the two Kappa distributions differ from the Maxwellian distribution, Fig. 2 shows a comparison between the Maxwellian, the modified Kappa, and the 145 standard Kappa distributions. The first thing we can notice is that both the modified and the standard Kappa distributions have higher-energy tails than the Maxwellian distribution, which is a defining characteristic of Kappa distributions. At the same time, we can also observe differences in the shape of each distribution, which are directly related to the effective temperature. In the standard Kappa distribution, the effective temperature  $T_\kappa$  is higher than that of both the Maxwellian and the modified Kappa distributions, as shown in equation 5. Consequently, the population of high-energy suprathermal particles (i.e., at large 150 velocity magnitudes) is significantly enhanced compared to the other distributions. At the same time, this increase in high-energy particles is accompanied by a reduction in the particle population within the low-energy core (i.e., at small velocity magnitudes). On the other hand, in the modified Kappa distribution, the effective temperature is the same as in the Maxwellian distribution.

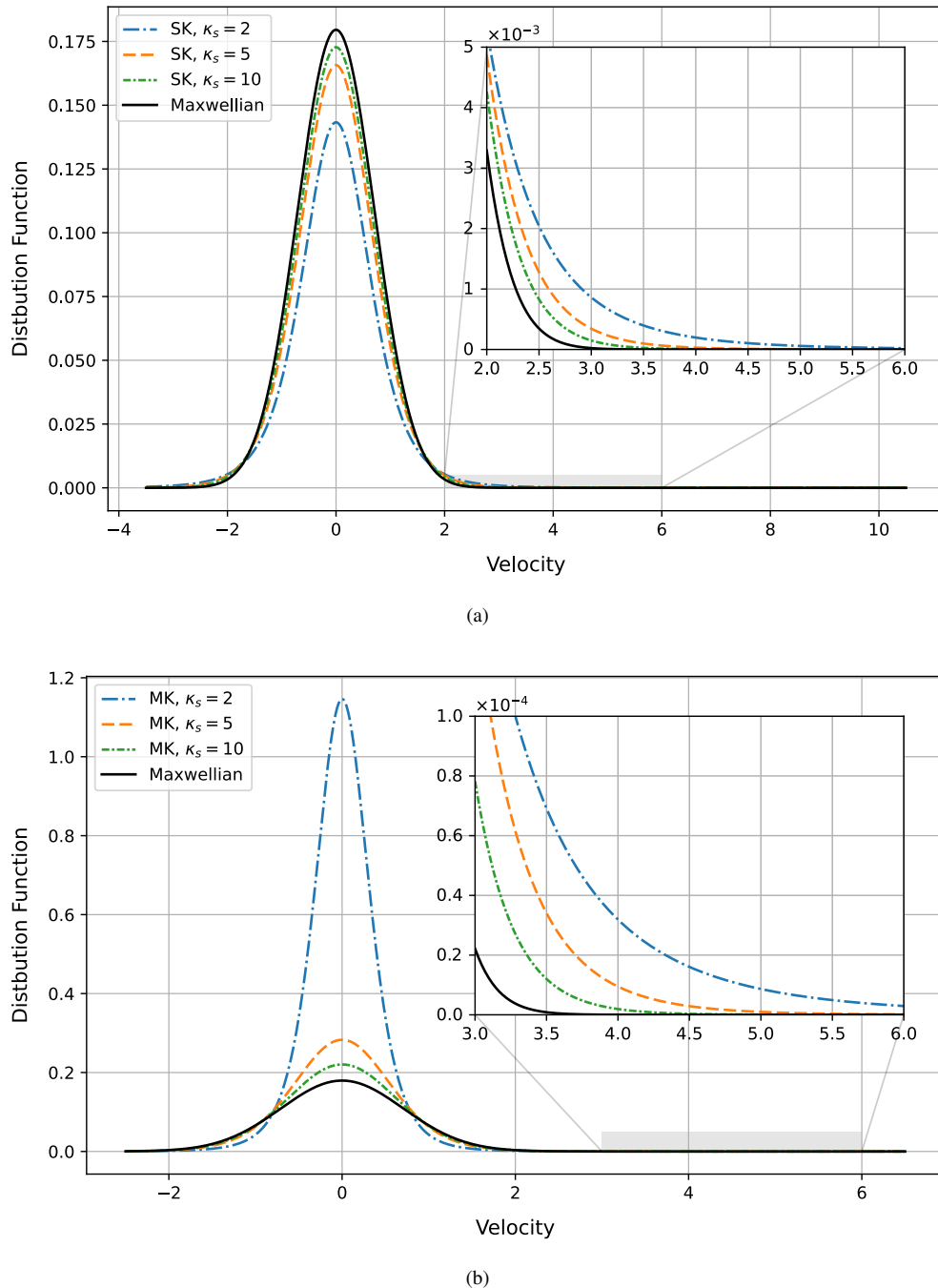


**Figure 1.** A schematic comparison between (a) standard Kappa, (b) modified Kappa velocity distributions for  $\kappa_s$  values 2, 5, and 10, with the Maxwellian velocity distribution.

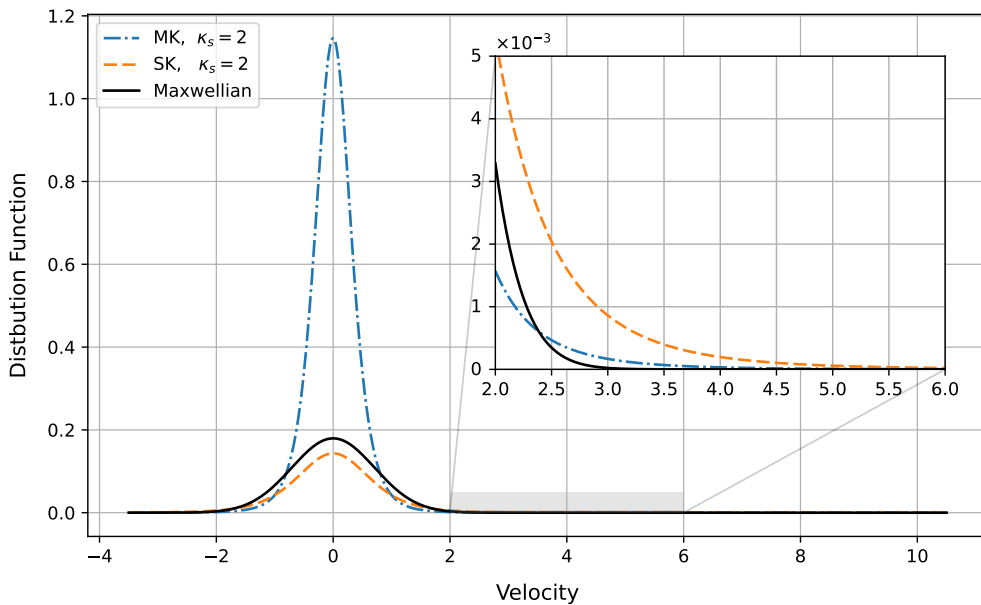


**Figure 2.** A schematic comparison of the standard Kappa distribution, the modified Kappa distribution for  $\kappa_s = 2$ , and the Maxwellian velocity distribution.

To maintain this equality in temperature, particles are redistributed between the low-energy core and the high-energy tail  
 155 without changing the system's total thermal energy. As a result, the high-energy tail of the modified Kappa distribution is lower than that of the standard Kappa distribution, while the particle population in the low-energy core becomes significantly higher.

Both the standard and modified Kappa distributions are used in different contexts. The standard Kappa distribution is the most commonly used tool in space plasma studies, where it provides excellent fits to spacecraft observations from the solar wind, planetary magnetospheres, and the heliosheath. It captures the empirical relationship between suprathermal particle  
 160 populations and the observed nonthermal heating of plasmas. On the other hand, the modified Kappa distribution, is mainly used in theoretical and statistical modeling, particularly in studies of systems governed by non-extensive entropy, long-range interactions, and quasi-stationary states. It provides a self-consistent description of plasma systems that exhibit deviations from classical thermodynamic equilibrium without requiring an increase in thermal energy.

Finally, Table 1 summarizes the main mathematical and physical properties of the Maxwellian, standard Kappa, and modified  
 165 Kappa velocity distribution functions discussed above, providing a compact overview of their key characteristics, parameter definitions, and limiting behavior, and allowing for an easy and direct comparison among the three distributions.



**Table 1.** Mathematical and physical comparison of Maxwellian, standard Kappa, and modified Kappa velocity distribution functions

Feature	Maxwellian (M)	Standard Kappa (SK)	Modified Kappa (MK)
Statistical nature	Thermal equilibrium	Non-equilibrium	Non-equilibrium
Theoretical basis	Boltzmann statistics	Empirical (space data)	Non-extensive statistics (Tsallis, 2012)
Primary application	Classical plasma theory	Space plasma fitting	Non-equilibrium plasma modeling with long-range interactions
Mathematical form	$f_s^M \propto \exp\left(\frac{c_s^2}{w_s^2}\right)$	$f_s^{SK} \propto (1 + (c_s^2/\kappa_s w_s^2))^{-\kappa_s - 1}$	$f_s^{MK} \propto (1 + (c_s^2/\kappa_{0s} w_s^2))^{-\kappa_s - 1}$
Normalization factor	$\frac{n_s}{\pi^{3/2} w_s^3}$	$\frac{n_s \kappa_s^{-3/2}}{\pi^{3/2} w_s^3} \frac{\Gamma(\kappa_s + 1)}{\Gamma(\kappa_s - 1/2)}$	$\frac{n_s \kappa_{0s}^{-3/2}}{\pi^{3/2} w_s^3} \frac{\Gamma(\kappa_s + 1)}{\Gamma(\kappa_s - 1/2)}$
Key shape parameter	—	$\kappa_s$	$\kappa_s, \kappa_{0s} = \kappa_s - 3/2$
Parameter constraint	—	$\kappa_s > 3/2$	$\kappa_s > 3/2$
Limit as $\kappa_s \rightarrow \infty$	—	Maxwellian distribution	Maxwellian distribution
Tail behavior	Exponential	Power-law	Power-law
Dominant region	Core-dominated	Tail-dominated	Core-dominated + tail
High-energy population	Lowest	Highest	Intermediate
Low-energy population	Intermediate	Lowest	Highest
Effective temperature	$T_\kappa = T_s$	$T_\kappa = \frac{\kappa_s}{\kappa_s - 3/2} T_s$	$T_\kappa = T_s$
Dependence of $T_\kappa$ on $\kappa_s$	Independent of $\kappa_s$	Increases as $\kappa_s$ decreases	Independent of $\kappa_s$
Total thermal energy	Baseline	Higher than Maxwellian	Same as Maxwellian

### 3 Theoretical Formulation

In this section, we derive the five-moment approximation of the system of transport equations, along with the corresponding collision terms and transport coefficients, using the standard Kappa distribution as the velocity distribution function. The 170 derivation follows the same mathematical framework and procedural steps established in Jwailes et al. (2025). While the full detailed calculations are not repeated here, the essential assumptions and methodological structure remain the same.

#### 3.1 Transport equations

The transport equations describe the spatial and temporal evolution of the physically significant velocity moments, such as number density, drift velocity, temperature, pressure tensor, stress tensor, and heat flow vector. These equations are obtained 175 by multiplying the Boltzmann equation by an appropriate velocity-dependent function and then integrating over the velocity space, as presented in Schunk (1977), Schunk and Nagy (2009), and Bittencourt (2004). The general transport equations do not constitute a closed system because the equation governing the moment of order  $l$  contains the moment of order  $l + 1$ . That is, while the continuity equation describes the evolution of the density, it also contains the drift velocity, and similar dependencies



occur in the higher-order moment equations. To close the system, the velocity distribution function  $f_s$ , is approximated by  
 180 expanding it into a complete orthogonal series around an appropriate zeroth-order distribution function  $f_s^{(0)}$ , which is chosen such that the series converges rapidly (Grad, 1949; Mintzer, 1965). When only the first term of this expansion is retained, the species distribution function  $f_s$ , is represented by the zeroth-order function,  $f_s^{(0)}$ . The general system of transport equations then reduces to the so-called five-moment approximation, in which the stress, heat flux, and all higher-order moments are neglected. At this level of approximation, the properties of each species are described by five parameters: the number density,  
 185 three components of drift velocity, and temperature. If the chosen zeroth-order distribution function  $f_s^{(0)}$  has a stress tensor  $\tau_s$  and a heat flux vector  $\mathbf{q}_s$  equal to zero, as in the drifting Maxwellian, drifting modified Kappa, and drifting standard Kappa distributions (Scherer et al., 2019), and if the main external forces acting on the charged particles are gravitational and Lorentz forces, the five-moment approximation equations become (Schunk, 1977),

$$\frac{\delta n_s}{\delta t} = \frac{\partial n_s}{\partial t} + \nabla \cdot (n_s \mathbf{u}_s), \quad (10)$$

$$\frac{\delta \mathbf{M}_s}{\delta t} = n_s m_s \frac{\mathbf{D}_s \mathbf{u}_s}{\mathbf{D}t} + \nabla p_s - n_s m_s \mathbf{G} - n_s e_s \left( \mathbf{E} + \frac{\mathbf{u}_s \times \mathbf{B}}{c} \right), \quad (11)$$

$$\frac{\delta E_s}{\delta t} = \frac{3}{2} \frac{\mathbf{D}_s p_s}{\mathbf{D}t} + \frac{5}{2} p_s (\nabla \cdot \mathbf{u}_s). \quad (12)$$

In these equations, the symbol  $\nabla$  denotes the gradient in coordinate space. The operator  $\mathbf{D}_s/\mathbf{D}t$ , is defined as

$$\frac{\mathbf{D}_s}{\mathbf{D}t} = \frac{\partial}{\partial t} + \mathbf{u}_s \cdot \nabla. \quad (13)$$

195 The partial pressure associated with this species is given by

$$p_s = n_s k_B T_s, \quad (14)$$

with  $n_s(\mathbf{r}, t)$  being the number density and  $T_s(\mathbf{r}, t)$  the temperature. The parameters  $e_s$  and  $m_s$  denote the charge and mass of species  $s$ , respectively. The vectors  $\mathbf{E}$  and  $\mathbf{B}$  correspond to the electric and magnetic fields, while  $\mathbf{G}$  represents the gravitational acceleration. Finally,  $c$  is the speed of light, and  $k_B$  stands for the Boltzmann constant.

200 **3.2 Collision terms**

The terms appearing on the left-hand side of the five-moment approximation, equations (10–12), are called the collision terms, also known as the transfer collision integral. These terms represent the moments of the Boltzmann collision integral and



describe the rate of change of density, momentum, and energy due to collisions, and they are defined as follows

$$\frac{\delta n_s}{\delta t} = \int_{\mathbb{R}^3} \frac{\delta f_s}{\delta t} d\mathbf{c}_s, \quad (15)$$

$$205 \quad \frac{\delta \mathbf{M}_s}{\delta t} = m_s \int_{\mathbb{R}^3} \mathbf{c}_s \frac{\delta f_s}{\delta t} d\mathbf{c}_s, \quad (16)$$

$$\frac{\delta E_s}{\delta t} = \frac{m_s}{2} \int_{\mathbb{R}^3} c_s^2 \frac{\delta f_s}{\delta t} d\mathbf{c}_s, \quad (17)$$

where the term  $(\delta f_s / \delta t)$ , represents the rate of change of the velocity distribution function  $f_s$ , in a given region of phase space as a result of collisions, and its form depends on the type of collision process considered. The appropriate expression in the case of binary elastic collisions between particles (collisions governed by inverse power laws, and resonant charge exchange 210 collisions) is the Boltzmann collision integral (Schunk, 1977; Schunk and Nagy, 2009), given by

$$\frac{\delta f_s}{\delta t} = \sum_t \int_{\mathbb{R}^3 \times \Omega} [f'_s f'_t - f_s f_t] g_{st} \sigma_{st}(g_{st}, \theta) d\Omega d\mathbf{c}_t, \quad (18)$$

where  $d\mathbf{c}_t$  is the random velocity space volume element for the target species  $t$ ,  $g_{st}$  is the magnitude of the relative velocity of the colliding particles  $s$  and  $t$ , with  $g_{st}$  defined as

$$\mathbf{g}_{st} = \mathbf{v}_s - \mathbf{v}_t, \quad (19)$$

215  $d\Omega$  is the element of solid angle in the  $s$  particle reference frame,  $\theta$  is the scattering angle,  $\sigma_{st}(g_{st}, \theta)$  is the differential scattering cross-section, defined as the number of particles scattered per solid angle  $d\Omega$ , per unit time, divided by the incident intensity, and the primes denote quantities evaluated after the collision. By evaluating the integrals appearing in equations (15–17), we obtain the general expressions for the collision terms under the assumption that the velocity distribution functions of both interacting species,  $s$  and  $t$ , follow drifting standard Kappa distributions. The results for the three types of collisions–Coulomb 220 collisions, hard-sphere interactions, and Maxwell molecule collisions–are summarized below.

$$\frac{\delta n_s}{\delta t} = 0, \quad (20)$$

$$\frac{\delta \mathbf{M}_s}{\delta t} = \sum_t n_s m_s \nu_{st}^{\text{SK}}(\kappa_s, \kappa_t) \Phi(\varepsilon_{st}) \Delta \mathbf{u}_{st}, \quad (21)$$

$$\frac{\delta E_s}{\delta t} = \sum_t n_s \left[ \frac{3}{2} k_B \nu_{st,T}^{\text{SK}}(\kappa_s, \kappa_t) \Psi(\varepsilon_{st}) \Delta T_{st}^{\text{SK}} \right. \\ \left. + m_{st} \nu_{st}^{\text{SK}}(\kappa_s, \kappa_t) \Phi(\varepsilon_{st}) |\Delta \mathbf{u}_{st}|^2 \right], \quad (22)$$

225 where the relative drift velocity  $\Delta \mathbf{u}_{st}$  and relative temperature difference  $\Delta T_{st}^{\text{SK}}$  are defined by

$$\Delta \mathbf{u}_{st} = \mathbf{u}_t - \mathbf{u}_s, \quad (23)$$

$$\Delta T_{st}^{\text{SK}} = H(\kappa_t) T_t - H(\kappa_s) T_s, \quad (24)$$



and the drift-to-thermal speed ratio  $\varepsilon_{st}$  is given by

$$\varepsilon_{st} = \frac{|\Delta \mathbf{u}_{st}|}{w_{st}}, \quad w_{st} = \sqrt{\frac{2k_B T_{st}}{m_{st}}}, \quad (25)$$

230 with the reduced mass  $m_{st}$  and the reduced temperature  $T_{st}$  are defined as

$$m_{st} = \frac{m_s m_t}{m_s + m_t}, \quad T_{st} = \frac{m_s T_s + m_t T_t}{m_s + m_t}. \quad (26)$$

The kappa-dependent terms  $\nu_{st}^{\text{SK}}$  and  $\nu_{st,T}^{\text{SK}}$  represent, respectively, the effective collision frequency and the thermal equilibration rate (or simply the thermalisation rate) for systems described by the standard Kappa distribution, and they are defined as

$$\nu_{st}^{\text{SK}}(\kappa_s, \kappa_t) = \nu_{st} D(\kappa_s, \kappa_t), \quad (27)$$

$$235 \quad \nu_{st,T}^{\text{SK}}(\kappa_s, \kappa_t) = 2 \frac{m_{st}}{m_t} \nu_{st}^{\text{SK}}, \quad (28)$$

where  $\nu_{st}$  denote the effective collision frequency rate for systems governed by the Maxwellian distribution. The factors  $\nu_{st}$ ,  $\Phi$ ,  $\Psi$ ,  $D$ , and  $H$  forms change depending on the type of collision, such as Coulomb, hard-sphere, or Maxwell molecule collisions, and can be summarized as follows:

*Coulomb collisions:*

240 The effective collision frequency for Coulomb collisions in the Maxwellian case is

$$\nu_{st} = \nu_{st}^{\text{Co}} = \frac{4}{3} \frac{n_t}{\pi^{1/2}} \frac{m_t}{m_s + m_t} \left( \frac{1}{2k_B} \frac{m_{st}}{T_{st}} \right)^{3/2} Q_{\text{Co}}, \quad (29)$$

where  $Q_{\text{Co}}$  is defined as

$$Q_{\text{Co}} = 4\pi \left( \frac{e_s e_t}{4\pi\epsilon_0 m_{st}} \right)^2 \ln \Lambda, \quad (30)$$

with  $e_s$  and  $e_t$  are the charges of species  $s$  and  $t$ , respectively,  $\epsilon_0$  is the permittivity of free space, and  $\ln \Lambda$  is the Coulomb 245 logarithm. The functions  $\Phi$  and  $\Psi$  are given by

$$\Phi = \Phi_{\text{Co}}(\varepsilon_{st}) = \frac{3\sqrt{\pi}}{4} \frac{\text{erf}(\varepsilon_{st})}{\varepsilon_{st}^3} - \frac{3e^{-\varepsilon_{st}^2}}{2\varepsilon_{st}^2}, \quad (31)$$

$$\Psi = \Psi_{\text{Co}}(\varepsilon_{st}) = e^{-\varepsilon_{st}^2}. \quad (32)$$

The kappa-dependent factors  $D$  and  $H$  are defined as

$$D(\kappa_s, \kappa_t) = \frac{(\kappa_s - 1/2)}{\kappa_s} \frac{(\kappa_t - 1/2)}{\kappa_t}, \quad (33)$$

$$250 \quad H(\kappa_\alpha) = \frac{\Gamma(\kappa_\alpha) \kappa_\alpha^{1/2}}{\Gamma(\kappa_\alpha + 1/2)}, \quad \alpha = s, t. \quad (34)$$



*Hard-sphere interactions:*

The effective collision frequency for Hard-sphere in the Maxwellian case is

$$\nu_{st} = \nu_{st}^{\text{HS}} = \frac{8}{3} \frac{n_t}{\pi^{1/2}} \frac{m_t}{m_s + m_t} \left( 2k_B \frac{T_{st}}{m_{st}} \right)^{1/2} Q_{\text{HS}}, \quad (35)$$

255 where  $Q_{\text{HS}}$  is defined as

$$Q_{\text{HS}} = \pi \sigma^2, \quad (36)$$

with  $\sigma$  represent the sum of the radii of the colliding particles. The functions  $\Phi$  and  $\Psi$  are given by

$$\begin{aligned} \Phi = \Phi_{\text{HS}}(\varepsilon_{st}) &= \frac{3}{8} \left( 1 + \frac{1}{2\varepsilon_{st}^2} \right) e^{-\varepsilon_{st}^2} \\ &+ \frac{3\sqrt{\pi}}{8} \left( \varepsilon_{st} + \frac{1}{\varepsilon_{st}} - \frac{1}{4\varepsilon_{st}^3} \right) \text{erf}(\varepsilon_{st}), \end{aligned} \quad (37)$$

$$260 \quad \Psi = \Psi_{\text{HS}}(\varepsilon_{st}) = \frac{\sqrt{\pi}}{2} \left( \varepsilon_{st} + \frac{1}{2\varepsilon_{st}} \right) \text{erf}(\varepsilon_{st}) + \frac{e^{-\varepsilon_{st}^2}}{2}. \quad (38)$$

The kappa-dependent factors D and H are defined the same as in equation (33) and (34).

*Maxwell molecule collisions*

The effective collision frequency for Maxwell molecule collisions in the Maxwellian case is

$$\nu_{st} = \nu_{st}^{\text{MC}} = \frac{n_t m_t}{m_s + m_t} Q_{\text{MC}}, \quad (39)$$

265 where  $Q_{\text{MC}}$  is defined as.

$$Q_{\text{MC}} = 0.844 \pi \left( \frac{K_{st}}{m_{st}} \right)^{1/2}, \quad (40)$$

with  $K_{st}$  denotes a proportionality constant that measures the force magnitude between particles. The functions  $\Phi$  and  $\Psi$  are given by

$$\Phi = \Phi_{\text{MC}}(\varepsilon_{st}) = 1, \quad \Psi = \Psi_{\text{MC}}(\varepsilon_{st}) = 1, \quad (41)$$

270 The factors D and H are defined as

$$D(\kappa_s, \kappa_t) = 1, \quad (42)$$

$$H(\kappa_\alpha) = \frac{\kappa_\alpha}{(\kappa_\alpha - 3/2)}, \quad \alpha = s, t. \quad (43)$$

A few remarks related to the collision terms summarized above are worth noting. First, the collision terms for non-drifting standard Kappa distributions can be obtained by setting the drift velocities of both interacting particles  $s$  and  $t$  to zero,  $\mathbf{u}_s =$



275  $\mathbf{u}_t = 0$ , in equations (20–22). The same result holds when the drift velocities of species  $s$  and  $t$  are equal, i.e.,  $\mathbf{u}_s = \mathbf{u}_t$ . Second, the functions  $\Phi$ 's and  $\Psi$ 's in case of Coulomb collision and hard sphere interaction, given in equations (31, 32, 37, and 38) can be written in terms of the hypergeometric functions, as discussed in Jwailes et al. (2025). Third, in the limit as  $\kappa$  approaches infinity,  $\kappa = \kappa_s = \kappa_t$ , the collision terms, equation (20–22), exactly recover the same results as those for the Maxwellian distribution (Schunk and Nagy, 2009), with the same definitions of  $\Phi$ ,  $\Psi$ , and  $\nu_{st}$ . That is, the effective collision frequency, the  
 280 thermalisation rate, and the relative temperature difference, which are the terms that the collision terms depend on the kappa parameter through, reduce to their form in the Maxwellian case

$$\lim_{\kappa \rightarrow \infty} \nu_{st}^{\text{SK}}(\kappa, \kappa) = \nu_{st}, \quad (44)$$

$$\lim_{\kappa \rightarrow \infty} \nu_{st,T}^{\text{SK}}(\kappa, \kappa) = \nu_{st,T}, \quad (45)$$

$$\lim_{\kappa \rightarrow \infty} \Delta T_{st}^{\text{SK}} = T_t - T_s = \Delta T_{st}. \quad (46)$$

285 Hence,

$$\lim_{\kappa \rightarrow \infty} D(\kappa, \kappa) = \lim_{\kappa \rightarrow \infty} H(\kappa) = 1. \quad (47)$$

With  $\nu_{st,T}$  denoting the thermalisation rate for systems governed by the Maxwellian distribution, defined as

$$\nu_{st,T} = 2 \frac{m_{st}}{m_t} \nu_{st}. \quad (48)$$

Obtaining the Maxwellian result provides a consistency check that the derived collision terms are correct, since the standard  
 290 Kappa distribution reduces to a Maxwellian distribution when the kappa parameter  $\kappa$  approaches infinity, as discussed in Section 2.

### 3.3 Transport coefficients

A Lorentz plasma is a type of plasma characterized by negligible electron–electron collisions compared to electron–ion collisions, allowing the electrons to be treated as moving through a background of nearly stationary ions (Du, 2013). In this setting, 295 and adopting the standard Kappa distribution, the transport coefficients—namely, the electrical conductivity  $\sigma_e$ , thermoelectric coefficient  $\alpha_e$ , diffusion coefficient  $D_e$ , and mobility coefficient  $\mu_e$ —can be derived using the five-moment approximation. The procedure starts from the momentum equation with a drifting standard Kappa distribution, equation (21), for a simple electron–ion collision. That is, by assuming a steady and low-inertia regime, unmagnetized plasma ( $\mathbf{B} = 0$ ) with negligible gravitational effects ( $\mathbf{G} = 0$ ), negligible ion drift ( $\mathbf{u}_i \approx 0$ ), and the electron drift velocity is small compared to the thermal 300 velocity ( $\epsilon_{ei} = 0$ ), the electron momentum equation reduces to the following form (Jwailes et al., 2025),

$$-n_e \mathbf{u}_e = \frac{k_B T_e}{m_e \nu_{ei}^{\text{SK}}} \nabla n_e + \frac{n_e k_B}{m_e \nu_{ei}^{\text{SK}}} \nabla T_e + \frac{n_e e}{m_e \nu_{ei}^{\text{SK}}} \mathbf{E}. \quad (49)$$

By setting  $\nabla n_e = 0$ , as in Husidic et al. (2021), equation 49 reduces to the generalized Ohm's law :

$$\mathbf{E} = \frac{\mathbf{J}_e}{\sigma_e} + \alpha_e \nabla T_e. \quad (50)$$



where  $\mathbf{E}$  denotes the electric field and  $\mathbf{J}_e$  is the current density, with  $e$  being the electron charge and  $n_e$  the electron number density. From this, we can identify the electrical conductivity and thermoelectric coefficient as

$$\sigma_e = \frac{n_e e^2}{m_e \nu_{ei}^{\text{SK}}}, \quad (51)$$

$$\alpha_e = -\frac{k_B}{e}. \quad (52)$$

Alternatively, by setting  $\nabla T_e = 0$ , as in Husidic et al. (2021), we obtain the extended Fick's law :

$$\Gamma_e = -D_e \nabla n_e - \mu_e n_e \mathbf{E}. \quad (53)$$

where  $\Gamma_e$  denotes the particle flux density, and the diffusion and mobility coefficients are identified as

$$D_e = \frac{k_B T_e}{m_e \nu_{ei}^{\text{SK}}}, \quad (54)$$

$$\mu_e = \frac{e}{m_e \nu_{ei}^{\text{SK}}}. \quad (55)$$

Equations 51, 52, 54, and 55 represent the mathematical forms of the transport coefficients governing electron dynamics in a Lorentz plasma with a standard Kappa distribution. Together, they demonstrate that electrical conduction, thermoelectric effects, diffusion, and mobility coefficients are controlled primarily by the electron-ion collision frequency.

## 4 Comparison of collision processes and transport coefficients

In this section, we present a comprehensive comparison of the results derived in Section 3 for three types of distributions: the standard Kappa, modified Kappa, and Maxwellian distributions. The comparison focuses on three aspects. First, we examine the effective collision frequency and the thermalisation rate. Next, we analyze the collision terms, specifically for Coulomb collisions. Finally, we compare the resulting transport coefficients for each distribution.

### 4.1 Effective collision frequency and thermalisation rate

The effective collision frequency describes the average rate of how frequently collisions occur, determining the efficiency of momentum transfer within the system, while the thermalisation rate measures how rapidly the system approaches thermal equilibrium through collisions. Both quantities are essential for understanding the exchange of momentum and energy between particles due to collisions. Within the five-moment approximation of the transport equations, these quantities are obtained directly from the momentum and energy collision terms. Expressions for the standard Kappa distribution are given in equations (27) and (28). Corresponding expressions for the modified Kappa distribution can be found in Jwailes et al. (2025), while those for the Maxwellian distribution are provided in Schunk and Nagy (2009).

Equations (27) and (28) show that, for the standard Kappa distribution, both the effective collision frequency and the thermalisation rate are affected by the kappa-dependent function  $D(\kappa_s, \kappa_t)$ . This function depends on the kappa parameters  $\kappa_s$  and



$\kappa_t$  of the interacting species  $s$  and  $t$  and its form varies with the type of collision process considered. In collision processes such as Maxwell molecule interactions, where the collision frequency is independent of particle velocity, the redistribution of particles' velocities introduced by the standard Kappa distribution has no effect. In this case,  $D = 1$ , and both the effective collision frequency and the thermalisation rate remain identical to the Maxwellian case,

335  $\nu_{st}^{\text{SK}} = \nu_{st}$ , and  $\nu_{st,T}^{\text{SK}} = \nu_{st,T}$ . (56)

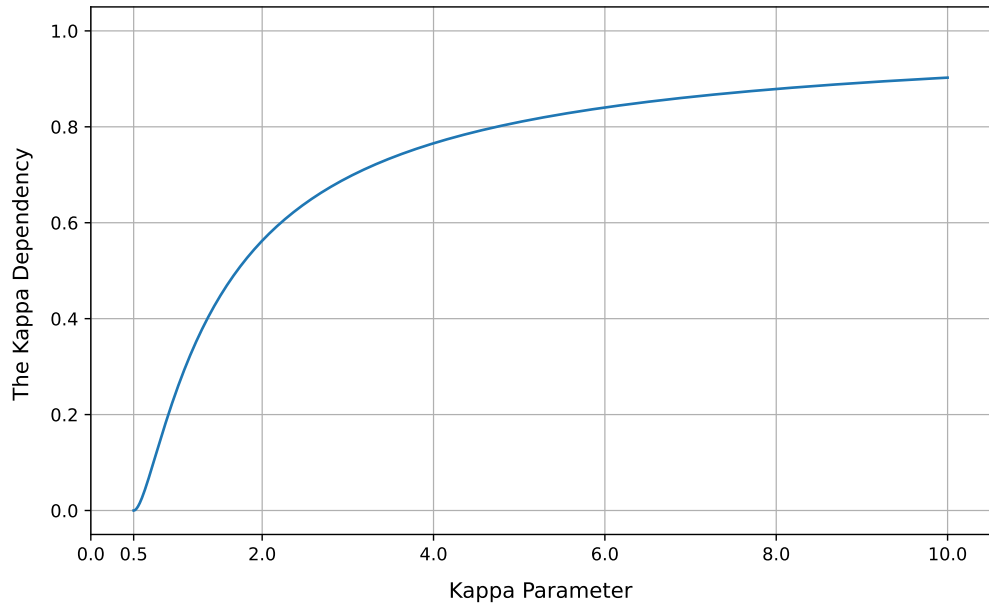


**Figure 3.** The kappa dependency for both the effective collision frequency and the thermalisation rate.

In contrast, for collision processes that strongly depend on particle velocity, the standard Kappa distribution significantly affects both the effective collision frequency and the thermalisation rate. This effect becomes particularly evident in processes such as Coulomb collisions and hard-sphere interactions, where the velocity distribution plays a central role. In these cases, 340 the function  $D$  vary according to the kappa parameters  $\kappa_s$  and  $\kappa_t$ , as given in equation (33). To compare the effective collision frequency and thermalisation rate with the Maxwellian case, and to better understand their behaviour, we consider the special case  $\kappa = \kappa_s = \kappa_t$ , so that the expressions,  $\nu_{st}^{\text{SK}}$  and  $\nu_{st,T}^{\text{SK}}$ , reduce to

$$\nu_{st}^{\text{SK}} = \nu_{st} \left( \frac{\kappa - 1/2}{\kappa} \right)^2, \quad (57)$$

$$\nu_{st,T}^{\text{SK}} = 2 \frac{m_{st}}{m_t} \nu_{st}^{\text{SK}}, \quad (58)$$



345 Equations (57) and (58) show that both the effective collision frequency and the thermalisation rate are reduced at low values of  $\kappa$  and increase as  $\kappa$  increases. As  $\kappa$  goes to infinity, the kappa term in equation (57) approaches 1, and the results converge to those of the Maxwellian distribution, as illustrated in Figure 3. In this figure, we plot the kappa dependency for both the effective collision frequency and the thermalisation rate; in other words, the ratios  $\nu_{st}^{\text{SK}}/\nu_{st}$  and  $\nu_{st,T}^{\text{SK}}/\nu_{st,T}$  as functions of the kappa parameter. This behaviour arises from the redistribution of the particles' velocities in the standard Kappa distribution.

350 As discussed in Section 2, low values of  $\kappa$  correspond to a reduced in the population of particles near the core with a small velocity magnitude compared to a Maxwellian distribution. Since collision frequency in Coulomb collision and hard sphere interactions are inversely proportional to function of velocity, this reduction leads to lower effective collision frequency and thermalisation rates at small  $\kappa$  values.

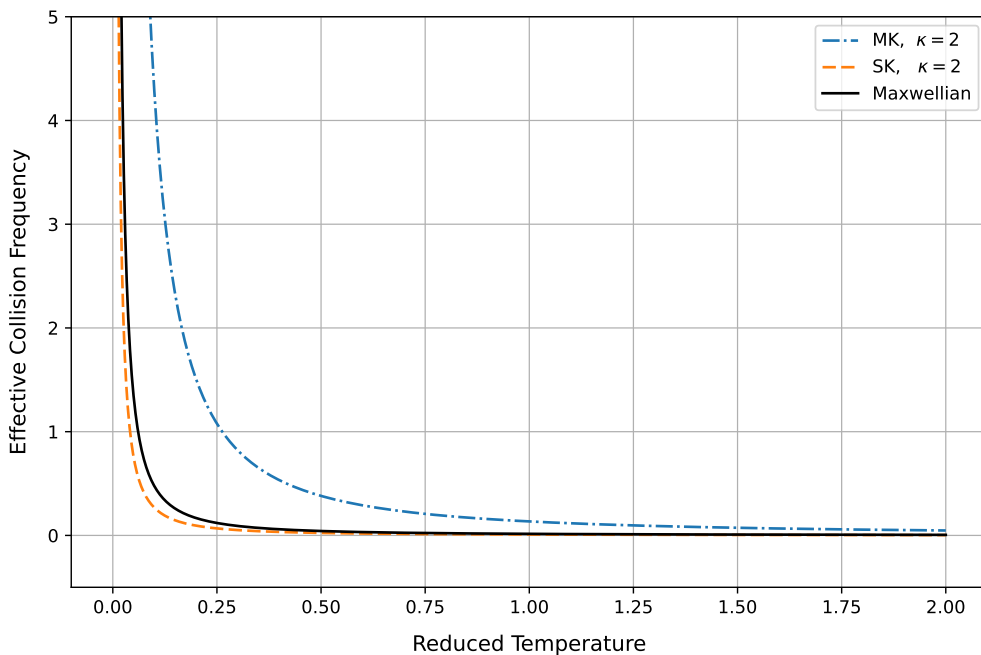


**Figure 4.** The effective collision frequency as a function of reduced temperature  $T_{st}$  for the Maxwellian, modified Kappa, and standard Kappa distributions.

355 For the modified Kappa distribution, Jwailes et al. (2025) derived both the effective collision frequency and the thermalisation rate. Since both the standard and the modified Kappa distributions primarily redistribute particles' velocities, the effective collision frequency remains unchanged when the collision frequency is independent of velocity. This is the case for Maxwell molecule interaction, for which the collision frequency is constant across Maxwellian, standard Kappa, and modified Kappa distributions

$$\nu_{st}^{\text{SK}} = \nu_{st}^{\text{MK}} = \nu_{st}, \quad \text{and} \quad \nu_{st,T}^{\text{SK}} = \nu_{st,T}^{\text{MK}} = \nu_{st,T}. \quad (59)$$



360 where  $\nu_{st}^{\text{MK}}$  and  $\nu_{st,T}^{\text{MK}}$  represent the effective collision frequency and the thermalisation rate, respectively, for systems described by the modified Kappa distribution. For collisions in which the collision frequency depends on particle velocity, such as Coulomb collisions or hard-sphere interactions, the choice of distribution strongly affects the effective collision frequency and the thermalisation rate. As discussed earlier, in the standard Kappa distribution, low values of  $\kappa$  lead to a reduced effective collision frequency compared to the Maxwellian case. However, this is not the case for the modified Kappa distribution, which 365 predicts the opposite behaviour, showing an increased effective collision frequency at low  $\kappa$  values. Figure 4 illustrates this behaviour by showing the effective collision frequency as a function of reduced temperature in the case of Coulomb collision for Maxwellian, standard Kappa, and modified Kappa distributions. The figure shows that all three distributions exhibit the same general behaviour. However, the standard Kappa distribution shows a lower effective collision frequency compared to the Maxwellian distribution, while the modified Kappa distribution shows a significantly higher effective collisions frequency 370 relative to the Maxwellian case. This behaviour arises from the redistribution of particle velocities in the standard and modified Kappa distributions, as discussed in Section 2. At low  $\kappa$  values, the low number of particles near the low energy core in the standard Kappa distribution leads to a lower effective collision frequency and thermalisation rate compared to the Maxwellian case. For the modified Kappa distribution, the number of particles near the core with small velocity magnitudes is higher than in the Maxwellian distribution, which increases the collision frequency for Coulomb collisions and hard sphere interactions.

375 **4.2 Collision terms**

The collision terms for the five-moment approximation, presented in equations (20–22), describe how the density, momentum, and energy for species  $s$  change due to collisions. These terms depend on, the number density  $n_s$ , drift velocity  $\mathbf{u}_s$ , and temperature  $T_s$  for species  $s$ , as well as on the the corresponding parameters of species  $t$ , number density  $n_t$ , drift velocity  $\mathbf{u}_t$ , and temperature  $T_t$ . Additionally, two functions of  $\kappa_s$  and  $\kappa_t$ , namely  $D(\kappa_s, \kappa_t)$  and  $H(\kappa_\alpha)$ ,  $\alpha = s, t$ , which contribute to the 380 effective collision frequency, the thermalisation rate, and the relative temperature difference. The particle masses  $m_s$  and  $m_t$  are constant and remain unchanged throughout the collision process for all types of collisions; as a result, the density collision term vanishes, as shown in equation (20).

In the Maxwellian case, both functions  $D(\kappa_s, \kappa_t)$  and  $H(\kappa_\alpha)$ ,  $\alpha = s, t$ , are set equal to one; see Sub-subsection 3.2. The behaviour of the momentum and energy collision terms in this case was studied in detail by Jwailes et al. (2025), providing an 385 explanation for the physical trends shown in Figures 5a and 5b. Figure 5a shows the isolines of the magnitude of the momentum collision term, assuming that the direction of  $\Delta\mathbf{u}_{st}$  along the  $z$ -axis, while Figure 5b shows the isolines of the corresponding energy collision term. Both figures display the dependence on  $\Delta\mathbf{u}_{st}$  and  $T_s$ , with all other constants set to 1.0 for simplicity. Assuming identical parameters for all  $t$  particles, the summation over  $t$  in equations (20–22) reduces to multiplication by their number,  $N_t$ , which is set to 1000 for the sake of comparison with other cases.

390 To understand how the standard Kappa distribution changes the collision terms, we plot the isolines of the momentum and energy collision terms as functions of  $\Delta\mathbf{u}_{st}$  and  $T_s$ , as shown in Figure 6. We assume equal kappa values for both species,  $s$  and  $t$ , i.e.,  $\kappa_s = \kappa_t = \kappa$ , to allow a direct comparison with the Maxwellian case and under the same conditions as in Figure 5a. The corresponding cross-sections at  $T_s = 0$  are shown in Figure 7. For the momentum collision term, the behavior closely



follows the Maxwellian case, with  $D(\kappa, \kappa)$  scaling the effective collision frequency, as shown in Figures 6 and 7. At low  $\kappa$ , the  
 395 effective collision frequency decreases, as discussed in Sub-subsection 4.1, leading to reduced momentum transfer.

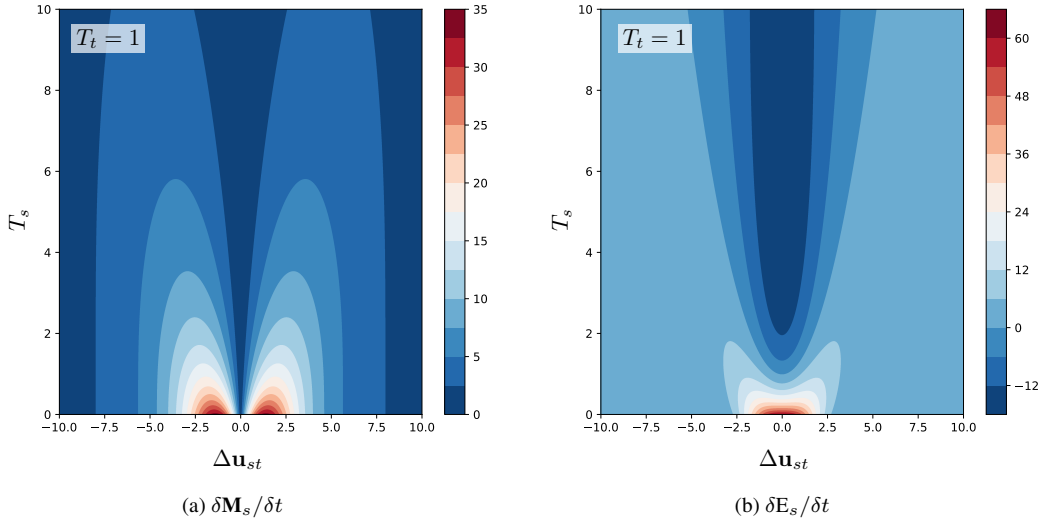


**Figure 5.** The momentum (a) and energy (b) collision terms for the Maxwellian velocity distribution function in the case of Coulomb collisions.

For the energy collision term, the function

$$W(\kappa, \kappa) = D(\kappa, \kappa) H(\kappa) \quad (60)$$

appears in the first term of equation 22, while  $D(\kappa, \kappa)$  contributes to the second term. The overall behavior is similar to the  
 400 Maxwellian case, with smaller values of  $\kappa$  yielding a smaller energy collision term. Overall, both collision terms increase with increasing  $\kappa$ , converging toward the Maxwellian result.

For the modified Kappa distribution, Jwailes et al. (2025) have studied the behavior of the collision term and compared it with that of the Maxwellian distribution under the same conditions previously applied to the standard Kappa distribution. The results show that the collision terms behave similarly to the standard Kappa and the Maxwellian distribution; however, the modified Kappa distribution amplifies the collision terms at low values of  $\kappa$ . That is, collisions have a stronger influence on  
 405 momentum and energy exchange between particles due to Coulomb interactions, which is the opposite behavior of the standard Kappa distribution discussed earlier. This significant difference is shown in Figure 8, which presents the cross sections of the momentum and energy collision terms at  $T_s = 0$  as functions of  $\Delta u_{st}$ . It is clear that, at the same value of  $\kappa$ , the collision terms in the modified Kappa distribution are much larger than those in both the standard Kappa and the Maxwellian distributions. This behavior is consistent with the results of Sub-section 4.1, where we found that the effective collision frequency and the  
 410 thermalization rate are significantly higher for the modified Kappa distribution than for the standard Kappa distribution, as a result of how the particles distribute near the core.

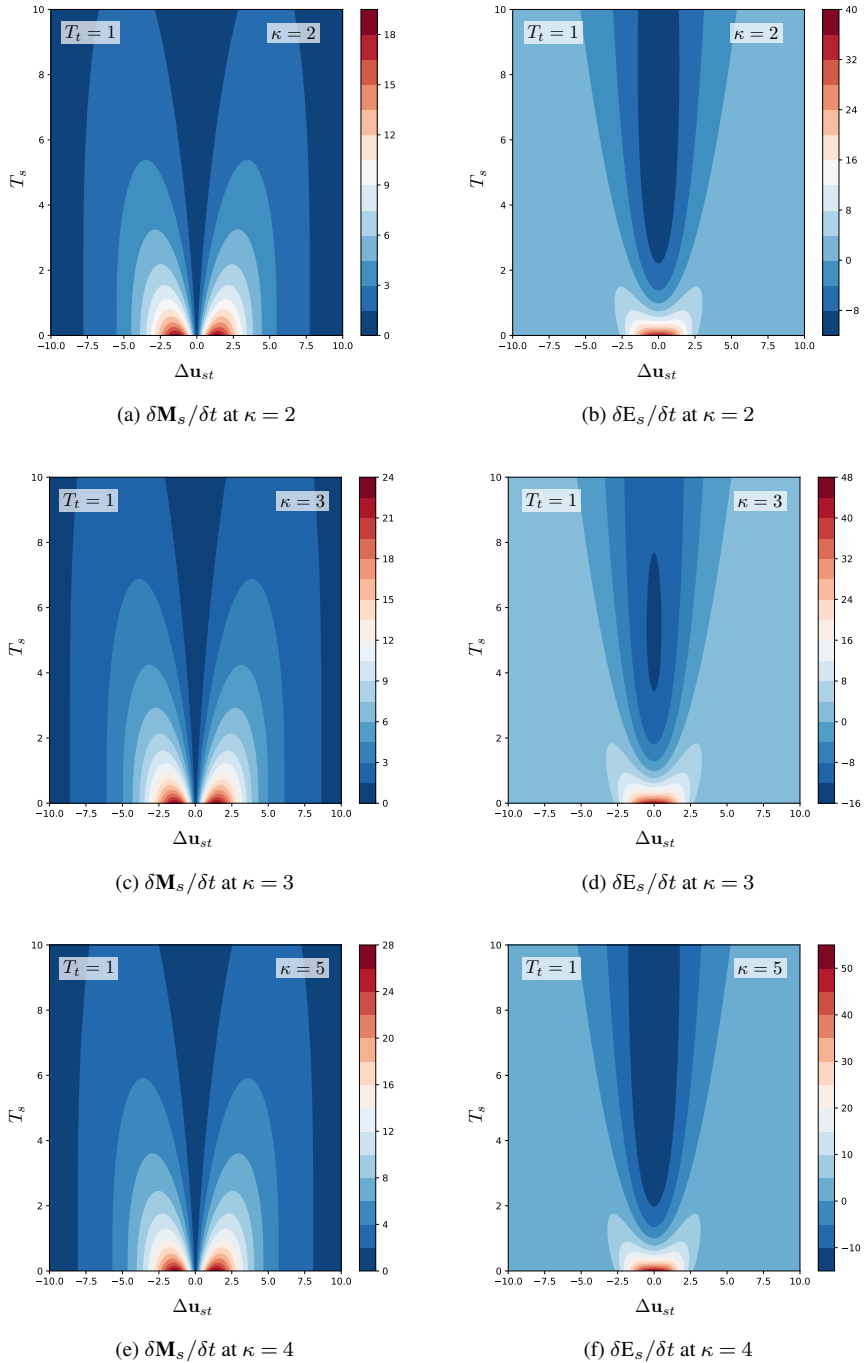
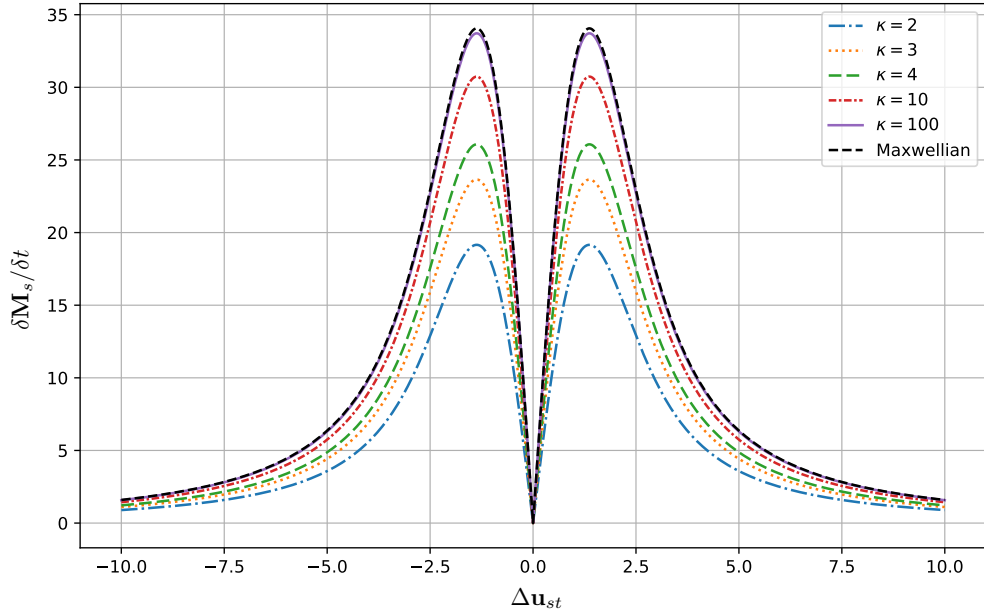
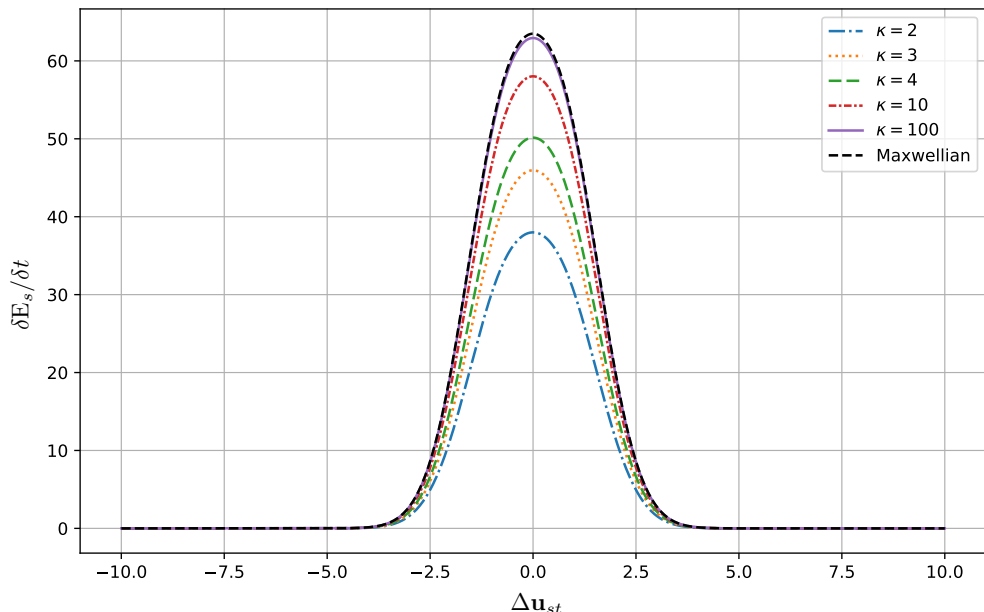


**Figure 6.** The momentum (a, c, e) and energy (b, d, f) collision terms for the standard Kappa velocity distribution function in the case of Coulomb collisions at different values of  $\kappa$ : 2, 3, and 4.



(a)  $\delta\mathbf{M}_s/\delta t$  at  $T_s = 0$



(b)  $\delta\mathbf{E}_s/\delta t$  at  $T_s = 0$

**Figure 7.** The cross-section of the momentum and energy collision terms for the standard Kappa and Maxwellian velocity distribution functions in the case of Coulomb collisions at  $T_s = 0$ .

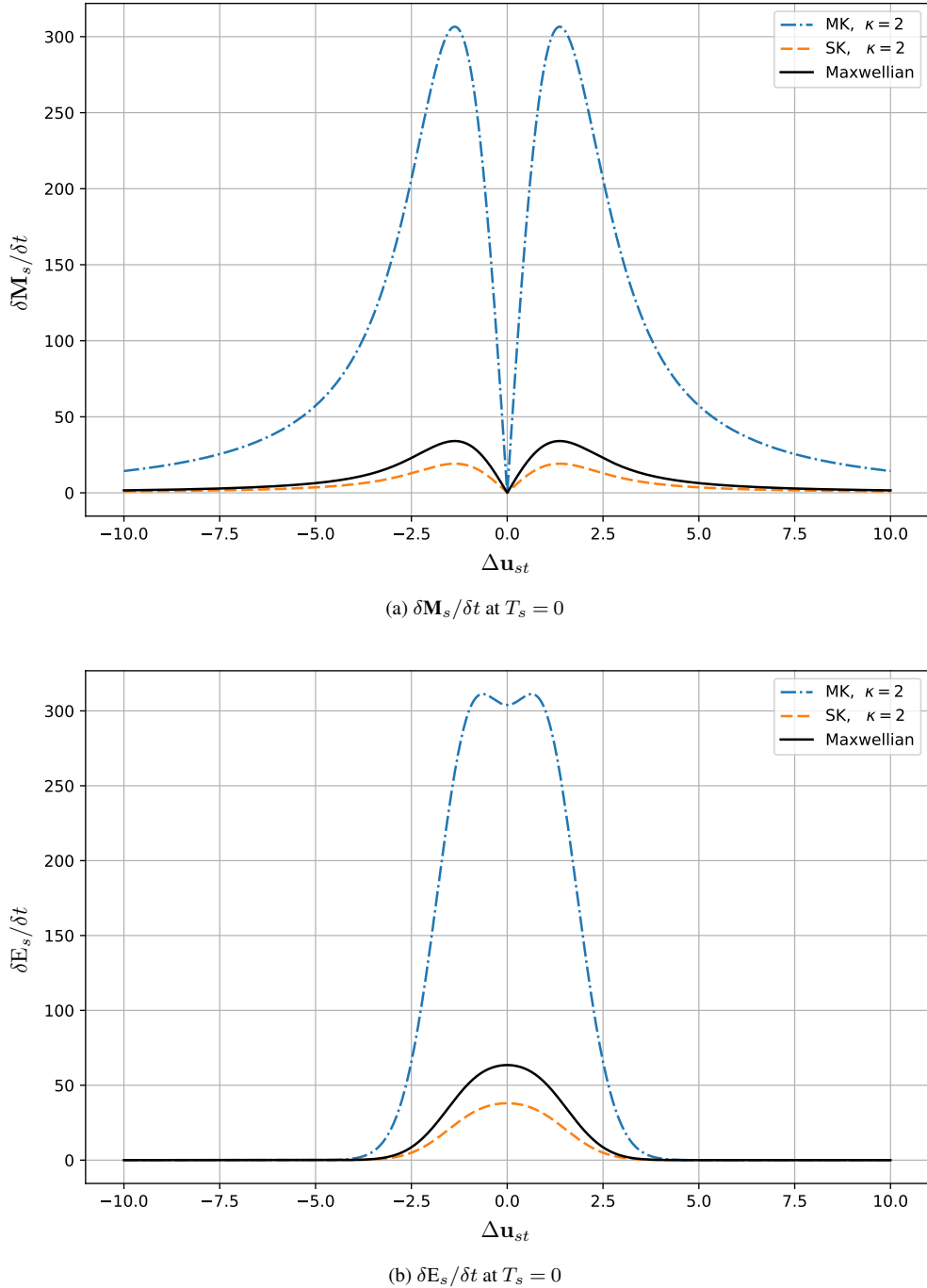


**Figure 8.** The cross-section of the momentum and energy collision terms for the standard Kappa and Maxwellian velocity distribution functions in the case of Coulomb collisions at  $T_s = 0$ .



### 4.3 Transport coefficients

From the first look at the derived expressions for the transport coefficients equation, electrical conductivity thermoelectric coefficient the diffusion and mobility coefficients listed in equations (51), (52), (54) and (55) respectively, we can see that they  
 415 satisfy the familiar relation between the electric conductivity and the mobility coefficient

$$\sigma_e = n_e e \mu_e, \quad (61)$$

and Einstein relation

$$D_e = \frac{k_B T_e}{e} \mu_e. \quad (62)$$

Importantly, both relations are found to hold consistently across all three considered velocity distributions: the standard Kappa,  
 420 the modified Kappa, and the Maxwellian distributions.

The resulting transport coefficients for the standard Kappa distribution exhibit distinct dependencies on the kappa parameters. In particular, the thermoelectric coefficient  $\alpha_e$  is independent of the kappa parameters, whereas the electrical conductivity, diffusion, and mobility all include the same kappa dependence through the effective collision frequency  $v_{ei}^{SK}$ . These transport coefficients are inversely proportional to the effective collision frequency. As discussed earlier, when  $\kappa = \kappa_s = \kappa_t$ , the effective  
 425 collision frequency affects different collision types in different ways. As a result, the influence of the standard Kappa distribution on the transport coefficients depends on the collision type. For Maxwell molecules, the effective collision frequency is identical to the Maxwellian case, and the transport coefficients remain unchanged. However, for Coulomb collisions and hard-sphere interactions, the effective collision frequency decreases as  $\kappa$  decreases, leading to an increase in the transport coefficients at low values of  $\kappa$  compared to the Maxwellian case, as shown in Figure 9, which shows the kappa dependence of the electrical  
 430 conductivity by plotting the ratio  $\sigma_e/\sigma_e^M$  as a function of  $\kappa$ , where  $\kappa = \kappa_t = \kappa_s$ , and

$$\sigma_e^M = \frac{n_e e^2}{m_e \nu_{ei}}. \quad (63)$$

As  $\kappa$  approaches infinity, the effective collision frequency  $v_{ei}^{SK}$  reduces to the Maxwellian case  $v_{ei}$ , making the transport coefficients recover their Maxwellian limits. In Figure 9, we also compare the dependence of the electrical conductivity on the  $\kappa$  parameter from the present study with the results reported by Husidic et al. (2021). While the figure shows a different dependence on the kappa parameter between the two studies, however, the overall behaviour is the same: at low  $\kappa$  values, the electrical conductivity becomes much larger than in the Maxwellian case, and as  $\kappa$  increases, we approach the Maxwellian case. This confirms that plasmas with smaller  $\kappa$  values conduct more efficiently. Thus, deviations from the Maxwellian limit lead to an increase in electrical conductivity. The difference in the kappa dependence arises from the collision models used in deriving the transport coefficients. While Husidic et al. (2021) employed a Krook-type (BGK) collision model, which provides  
 435 a simplified representation of collisions, our work uses the full Boltzmann collision integral, which offers a more realistic description, particularly for Coulomb collisions.

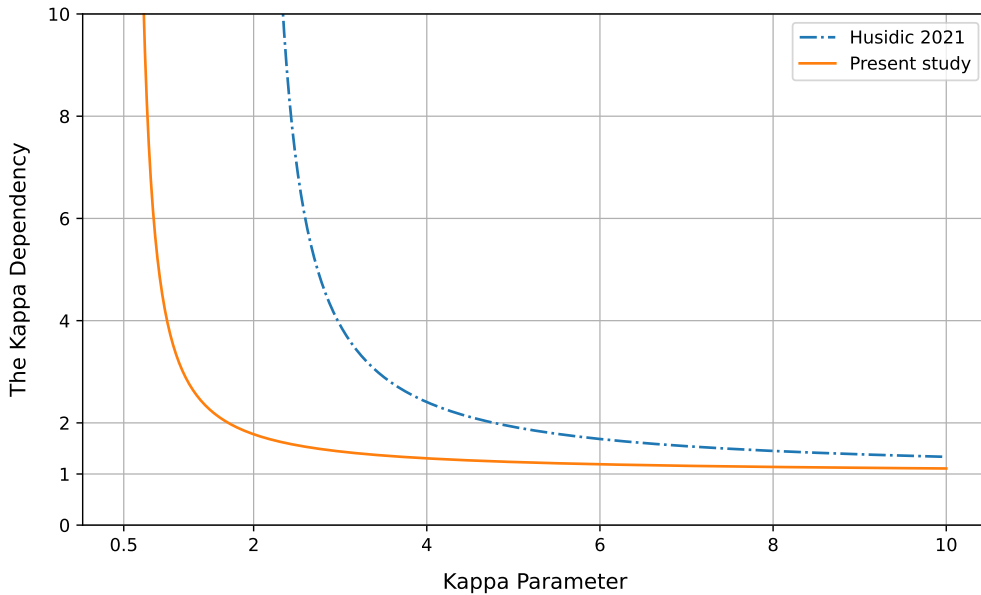


**Figure 9.** The kappa dependency for the electrical conductivity

For the modified Kappa distribution, the transport coefficients were derived by Jwailes et al. (2025). Similar to the standard Kappa distribution, the modified Kappa distribution does not affect the thermoelectric coefficients, and no dependence on the Kappa parameter appears. However, the remaining transport coefficients are influenced through the effective collision frequency, in the same way as for the standard Kappa and Maxwellian distributions. If the collision frequency is independent of particle velocity, the effective collision frequency remains unchanged, and the transport coefficients are identical for the Maxwellian, standard Kappa, and modified Kappa distributions. For collisions in which the collision frequency depends on particle velocity—such as Coulomb collisions or hard-sphere interactions—the effective collision frequency is affected by the modified Kappa distribution. As a result, the transport coefficients acquire a kappa-parameter dependence, where the transport coefficient at small kappa values becomes smaller than in the Maxwellian case. This behavior is opposite to that of the standard Kappa distribution, where, as mentioned earlier, small kappa values increase the transport coefficient relative to the Maxwellian case. Figure 10 illustrates this difference by plotting the electrical conductivity as a function of the reduced temperature for the three distributions—Maxwellian, modified Kappa, and standard Kappa. The figure shows that all three distributions exhibit the same general behavior; however, the standard Kappa distribution yields a higher electrical conductivity than the Maxwellian, while the modified Kappa distribution yields a lower value. This difference arises from the redistribution of particle velocities. At low  $\kappa$ , the standard Kappa distribution contains fewer particles in the low-energy core than the Maxwellian, reducing the collision frequency for interactions inversely proportional to velocity, such as Coulomb collisions and hard sphere interactions. This lowers the effective collision frequency and thermalisation rate at low  $\kappa$ . In contrast, the modified Kappa distribution increases the population of core particles, leading to higher collision frequencies for these interactions.

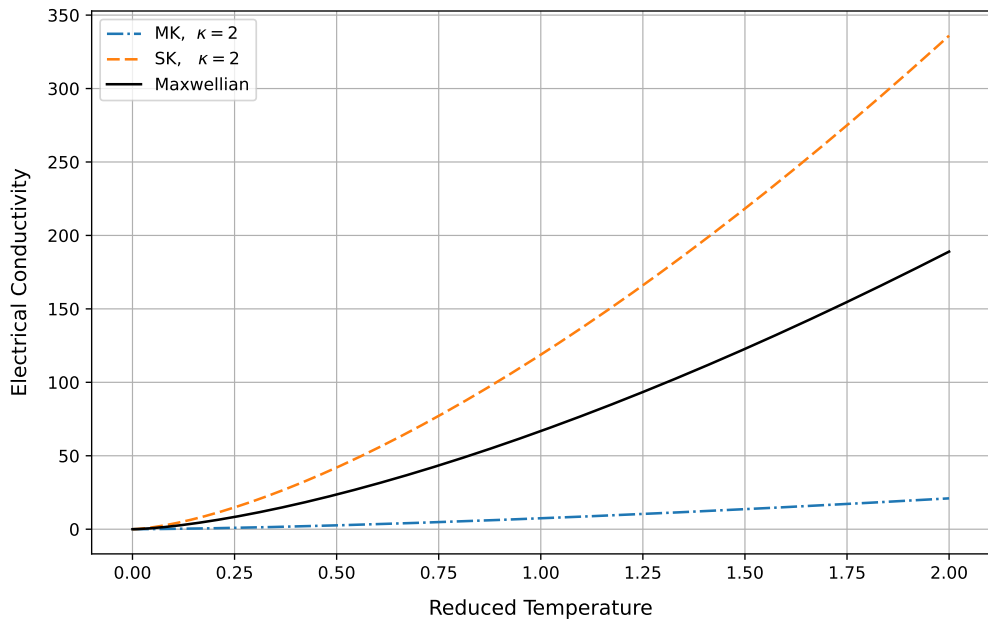


**Figure 10.** The electrical conductivity as a function of reduced temperature  $T_{st}$  for the Maxwellian, modified Kappa, and standard Kappa distributions.

460 Finally, Tables 2, 3 and 4 summarize the main mathematical expressions and low- $\kappa$  physical trends of the collision terms and transport coefficients for the Maxwellian, standard Kappa, and modified Kappa velocity distribution functions for the three types of collisions: Coulomb collisions, hard-sphere interactions, and Maxwell molecule interactions. The tables provide a compact side-by-side comparison of effective collision frequencies, thermalisation rates, momentum and energy exchange, and transport coefficients for both Coulomb collisions and Maxwell molecule interactions, highlighting similarities and differences  
465 among the three distributions.



**Table 2.** Mathematical and physical comparison between the Maxwellian, standard Kappa, and modified Kappa velocity distribution functions for Coulomb collisions

Feature / Aspect	Maxwellian (M)	Standard Kappa (SK)	Modified Kappa (MK)
Effective collision frequency	$\nu_{st}^{\text{Co}}$	$\nu_{st}^{\text{Co}} \left( \frac{\kappa - 1/2}{\kappa} \right)^2$	$\nu_{st}^{\text{Co}} \left( \frac{\kappa - 1/2}{\kappa - 3/2} \right)^2$
Effective collision frequency behavior at low $\kappa$	Baseline	Lower than Maxwellian	Higher than Maxwellian
Thermalisation rate	$\nu_{ei,T}^{\text{M}} = 2 \frac{m_{ei}}{m_i} \nu_{ei}^{\text{Co}}$	$\nu_{ei,T}^{\text{M}} \left( \frac{\kappa - 1/2}{\kappa} \right)^2$	$\nu_{ei,T}^{\text{M}} \left( \frac{\kappa - 1/2}{\kappa - 3/2} \right)^2$
Thermalisation rate behavior at low $\kappa$	Baseline	Lower than Maxwellian	Higher than Maxwellian
Momentum exchange at low $\kappa$	Baseline	Lower than Maxwellian	Higher than Maxwellian
Energy exchange at low $\kappa$	Baseline	Lower than Maxwellian	Higher than Maxwellian
Thermoelectric coefficient	$\alpha_e^{\text{M}} = -\frac{k_B}{e}$	$\alpha_e^{\text{M}}$	$\alpha_e^{\text{M}}$
Thermoelectric coefficient behavior at low $\kappa$	Baseline	Same as Maxwellian	Same as Maxwellian
Electrical conductivity	$\sigma_e^{\text{M}} = \frac{n_e e^2}{m_e \nu_{ei}^{\text{Co}}}$	$\sigma_e^{\text{M}} \left( \frac{\kappa}{\kappa - 1/2} \right)^2$	$\sigma_e^{\text{M}} \left( \frac{\kappa - 3/2}{\kappa - 1/2} \right)^2$
Electrical conductivity behavior at low $\kappa$	Baseline	Higher than Maxwellian	Lower than Maxwellian
Diffusion coefficient	$D_e^{\text{M}} = \frac{k_B T_e}{m_e \nu_{ei}^{\text{Co}}}$	$D_e^{\text{M}} \left( \frac{\kappa}{\kappa - 1/2} \right)^2$	$D_e^{\text{M}} \left( \frac{\kappa - 3/2}{\kappa - 1/2} \right)^2$
Diffusion coefficient behavior at low $\kappa$	Baseline	Higher than Maxwellian	Lower than Maxwellian
Mobility coefficient	$\mu_e^{\text{M}} = \frac{e}{m_e \nu_{ei}^{\text{Co}}}$	$\mu_e^{\text{M}} \left( \frac{\kappa}{\kappa - 1/2} \right)^2$	$\mu_e^{\text{M}} \left( \frac{\kappa - 3/2}{\kappa - 1/2} \right)^2$
Mobility coefficient behavior at low $\kappa$	Baseline	Higher than Maxwellian	Lower than Maxwellian



**Table 3.** Mathematical and physical comparison between the Maxwellian, standard Kappa, and modified Kappa velocity distribution functions for hard sphere interaction

Feature / Aspect	Maxwellian (M)	Standard Kappa (SK)	Modified Kappa (MK)
Effective collision frequency	$\nu_{st}^{\text{HS}}$	$\nu_{st}^{\text{HS}} \left( \frac{\kappa - 1/2}{\kappa} \right)^2$	$\nu_{st}^{\text{HS}} \left( \frac{\kappa - 1/2}{\kappa - 3/2} \right)^2$
Effective collision frequency behavior at low $\kappa$	Baseline	Lower than Maxwellian	Higher than Maxwellian
Thermalisation rate	$\nu_{ei,T}^{\text{M}} = 2 \frac{m_{ei}}{m_i} \nu_{ei}^{\text{HS}}$	$\nu_{ei,T}^{\text{M}} \left( \frac{\kappa - 1/2}{\kappa} \right)^2$	$\nu_{ei,T}^{\text{M}} \left( \frac{\kappa - 1/2}{\kappa - 3/2} \right)^2$
Thermalisation rate behavior at low $\kappa$	Baseline	Lower than Maxwellian	Higher than Maxwellian
Momentum exchange at low $\kappa$	Baseline	Lower than Maxwellian	Higher than Maxwellian
Energy exchange at low $\kappa$	Baseline	Lower than Maxwellian	Higher than Maxwellian
Thermoelectric coefficient	$\alpha_e^{\text{M}} = -\frac{k_B}{e}$	$\alpha_e^{\text{M}}$	$\alpha_e^{\text{M}}$
Thermoelectric coefficient behavior at low $\kappa$	Baseline	Same as Maxwellian	Same as Maxwellian
Electrical conductivity	$\sigma_e^{\text{M}} = \frac{n_e e^2}{m_e \nu_{ei}^{\text{HS}}}$	$\sigma_e^{\text{M}} \left( \frac{\kappa}{\kappa - 1/2} \right)^2$	$\sigma_e^{\text{M}} \left( \frac{\kappa - 3/2}{\kappa - 1/2} \right)^2$
Electrical conductivity behavior at low $\kappa$	Baseline	Higher than Maxwellian	Lower than Maxwellian
Diffusion coefficient	$D_e^{\text{M}} = \frac{k_B T_e}{m_e \nu_{ei}^{\text{HS}}}$	$D_e^{\text{M}} \left( \frac{\kappa}{\kappa - 1/2} \right)^2$	$D_e^{\text{M}} \left( \frac{\kappa - 3/2}{\kappa - 1/2} \right)^2$
Diffusion coefficient behavior at low $\kappa$	Baseline	Higher than Maxwellian	Lower than Maxwellian
Mobility coefficient	$\mu_e^{\text{M}} = \frac{e}{m_e \nu_{ei}^{\text{HS}}}$	$\mu_e^{\text{M}} \left( \frac{\kappa}{\kappa - 1/2} \right)^2$	$\mu_e^{\text{M}} \left( \frac{\kappa - 3/2}{\kappa - 1/2} \right)^2$
Mobility coefficient behavior at low $\kappa$	Baseline	Higher than Maxwellian	Lower than Maxwellian



**Table 4.** Mathematical and physical comparison between the Maxwellian, standard Kappa, and modified Kappa velocity distribution functions for Maxwell molecule interactions

Feature / Aspect	Maxwellian (M)	Standard Kappa (SK)	Modified Kappa (MK)
Effective collision frequency	$\nu_{ei}^{MC}$	$\nu_{ei}^{MC}$	$\nu_{ei}^{MC}$
Effective collision frequency behavior at low $\kappa$	Baseline	Same as Maxwellian	Same as Maxwellian
Thermalisation rate	$\nu_{ei,T}^M = 2 \frac{m_{ei}}{m_i} \nu_{ei}^{MC}$	$\nu_{ei,T}^M$	$\nu_{ei,T}^M$
Thermalisation rate behavior at low $\kappa$	Baseline	Same as Maxwellian	Same as Maxwellian
Momentum exchange at low $\kappa$	Baseline	Same as Maxwellian	Same as Maxwellian
Energy exchange at low $\kappa$	Baseline	Higher than Maxwellian	Same as Maxwellian
Thermoelectric coefficient	$\alpha_e^M = -\frac{k_B}{e}$	$\alpha_e^M$	$\alpha_e^M$
Thermoelectric coefficient behavior at low $\kappa$	Baseline	Same as Maxwellian	Same as Maxwellian
Electrical conductivity	$\sigma_e^M = \frac{n_e e^2}{m_e \nu_{ei}^{MC}}$	$\sigma_e^M$	$\sigma_e^M$
Conductivity conductivity behavior at low $\kappa$	Baseline	Same as Maxwellian	Same as Maxwellian
Diffusion coefficient	$D_e^M = \frac{k_B T_e}{m_e \nu_{ei}^{MC}}$	$D_e^M$	$D_e^M$
Diffusion coefficient behavior at low $\kappa$	Baseline	Same as Maxwellian	Same as Maxwellian
Mobility coefficient	$\mu_e^M = \frac{e}{m_e \nu_{ei}^{MC}}$	$\mu_e^M$	$\mu_e^M$
Mobility coefficient behavior at low $\kappa$	Baseline	Same as Maxwellian	Same as Maxwellian



## 5 Conclusions

For a Lorentz plasma described by a standard Kappa distribution, we derive expressions for the transport coefficients: electrical conductivity, thermoelectric, diffusion, and mobility. The analysis begins with a closed system of transport equations for isotropic plasmas within the five-moment approximation. Transport properties are defined relative to the random velocity of each species, with the velocity distribution function expanded in an orthogonal polynomial series about a drifting standard Kappa distribution. By taking only the first term and neglecting higher order moments yields the five-moment approximation. The corresponding momentum and energy collision terms are evaluated via the Boltzmann collision integral for several interaction types, including Coulomb collisions, hard-sphere interactions, and Maxwell molecule collisions. Under suitable assumptions for an unmagnetized, steady-state plasma, explicit expressions for the transport coefficients for the standard Kappa distribution are obtained from the momentum equation.

The methodology adopted in this study is broadly comparable to that of Jwailes et al. (2025), particularly in terms of the formulation of the transport equations, the evaluation of the collision integrals, and the derivation of the transport coefficients. However, a fundamental distinction between the two studies leads to markedly different physical outcomes. While Jwailes et al. (2025) employed a modified Kappa distribution function, the present work is based on the standard Kappa distribution. These two distributions differ substantially in their statistical representation of plasma particle populations, resulting in distinct plasma responses and transport properties. Although the mathematical forms of the governing equations appear similar, the physical interpretation of the quantities involved depends critically on the specific Kappa distribution adopted. This difference motivates the detailed comparative analysis presented in Section 4. That analysis compares three velocity distributions: Maxwellian, standard Kappa, and modified Kappa, across three stages. The first stage examined the effect of the kappa parameter on the effective collision frequency and the thermalisation rate. The second stage focused on how the kappa parameter affects the momentum and energy collision terms for Coulomb collisions. The third stage investigated the impact of the kappa parameter on transport coefficients, including electrical conductivity, diffusion, mobility, and the thermoelectric coefficient. The results of this comparison reveals that the standard Kappa distribution exhibits behavior that is qualitatively different from that of the modified Kappa distribution. For velocity-independent interactions, such as Maxwell molecules, the choice of velocity distribution does not affect the collision frequency or the thermalisation rate. Consequently, the transport coefficients remain identical across all three distributions. In contrast, for velocity-dependent interactions, including Coulomb and hard-sphere collisions, the effects of the kappa parameter become significant. In the standard Kappa distribution, low values of  $\kappa$  lead to a reduction in the effective collision frequency, the number of collisions, and the thermalisation rate. This reduction, in turn, results in enhanced transport coefficients. Conversely, in the modified Kappa distribution, low  $\kappa$  values increase the effective collision frequency and collision rates, which leads to a corresponding reduction in transport coefficients.

While this study advances non-Maxwellian transport theory, it has several limitations. The approach relies on the five-moment approximation, retaining only the first expansion term and neglecting higher-order moments that could affect system behavior. It assumes isotropic plasmas, limiting applicability to real space environments, where magnetization and temperature or pressure anisotropies are common. The Coulomb collision cross-section is simplified using a constant logarithm and



500 large-velocity approximation, reducing accuracy at low velocities (Fichtner et al., 1996). Additionally, the standard Kappa distribution becomes unphysical for  $\kappa \leq 3/2$ , as the kappa terms D and H diverge, making collision frequency and thermalization rate undefined, so the derived coefficients are valid only for  $\kappa > 3/2$ . Future work should address these limitations by developing a transport theory for the standard Kappa distribution via a generalized polynomial expansion, extending the theory to anisotropic plasmas, incorporating the exact velocity-dependent Coulomb cross-section, and adopting the Regularized Kappa  
505 Distribution (Scherer et al., 2017, 2019) to ensure finite moments and thermodynamic consistency.

*Code availability.* No external or third-party software code was used in this work beyond standard, widely available plotting functions provided by common scientific computing environments. The plotting routines applied in this study consist solely of simple function evaluations and visualizations based directly on the analytical formulas already presented in the paper. All formulas, computational steps, and expressions used to generate the figures are fully described within the paper itself. Because no custom or novel software code was developed and  
510 because the figures can be reproduced entirely from the equations provided, there is no separate software package to archive, cite, or deposit in a public repository.

*Data availability.* This study did not generate or use any external research data. All figures are produced directly from analytical formulas included within the paper, and no numerical datasets were created, collected, or processed. As such, no datasets exist to deposit in a public repository, and no data DOI or persistent URL is applicable.

515 *Author contributions.* M. J. Jwailes proposed the research idea, carried out the theoretical work, derived the framework used to obtain the figures and results, wrote the initial manuscript, and led the discussion of the findings. I. A. Barghouthi supervised the study, verified the validity of the results, and assisted in scientific editing of the manuscript. Q. S. Atawnah contributed to the final revisions of the manuscript.

*Competing interests.* The authors declare that they have no competing interests.

520 *Disclaimer.* The views expressed in this article are solely those of the authors and do not necessarily represent the views of their affiliated institutions.

*Acknowledgements.*



## References

Bittencourt, J.: Fundamentals of Plasma Physics, Springer New York, 3rd ed edn., 2004.

Collier, M. R. and Hamilton, D. C.: The relationship between kappa and temperature in energetic ion spectra at Jupiter, *Geophysical Research Letters*, 22, 303–306, <https://doi.org/10.1029/94GL02997>, 1995.

Davis, S., Avaria, G., Bora, B., Jain, J., Moreno, J., Pavez, C., and Soto, L.: Kappa distribution from particle correlations in nonequilibrium, steady-state plasmas, *Physical Review E*, 108, 065 207, <https://doi.org/10.1103/PhysRevE.108.065207>, 2023.

Du, J.: Transport coefficients in Lorentz plasmas with the power-law kappa-distribution, *Physics of Plasmas*, 20, 092 901, <https://doi.org/10.1063/1.4820799>, 2013.

Ebne Abbasi, Z. and Esfandyari-Kalejahi, A.: Transport coefficients of a weakly ionized plasma with nonextensive particles, *Physics of Plasmas*, 26, 012 301, <https://doi.org/10.1063/1.5051585>, 2019.

Ebne Abbasi, Z., Esfandyari-Kalejahi, A., and Khaledi, P.: The collision times and transport coefficients of a fully ionized plasma with superthermal particles, *Astrophysics and Space Science*, 362, 103, <https://doi.org/10.1007/s10509-017-3081-4>, 2017.

Fichtner, H., Sreenivas, S. R., and Vormbrock, N.: Transfer integrals for fully ionized gases, *Journal of Plasma Physics*, 55, 95–120, <https://doi.org/10.1017/S002237780018699>, 1996.

Formisano, V., Moreno, G., Palmiotti, F., and Hedgecock, P. C.: Solar Wind Interaction with the Earth's Magnetic Field 1. Magnetosheath, *Journal of Geophysical Research (1896-1977)*, 78, 3714–3730, <https://doi.org/10.1029/JA078i019p03714>, 1973.

Grad, H.: On the kinetic theory of rarefied gases, *Communications on Pure and Applied Mathematics*, 2, 331–407, <https://doi.org/10.1002/cpa.3160020403>, 1949.

Guo, R. and Du, J.: Transport coefficients of the fully ionized plasma with kappa-distribution and in strong magnetic field, *Physica A: Statistical Mechanics and its Applications*, 523, 156–171, <https://doi.org/10.1016/j.physa.2019.02.011>, 2019.

Husidic, E., Lazar, M., Fichtner, H., Scherer, K., and Poedts, S.: Transport coefficients enhanced by suprathermal particles in nonequilibrium heliospheric plasmas, *Astronomy & Astrophysics*, 654, A99, <https://doi.org/10.1051/0004-6361/202141760>, 2021.

Jwailes, M. J., Barghouthi, I. A., and Atawnah, Q. S.: Transport coefficients in modified Kappa distributed plasmas, *Annales Geophysicae*, 43, 783–802, <https://doi.org/10.5194/angeo-43-783-2025>, 2025.

Lazar, M. and Fichtner, H.: Kappa Distributions: From Observational Evidences via Controversial Predictions to a Consistent Theory of Nonequilibrium Plasmas, *Astrophysics and Space Science Library*, Springer International Publishing, ISBN 9783030826239, <https://books.google.ps/books?id=ZtNSEAAAQBAJ>, 2021.

Livadiotis, G.: Kappa distributions: Theory and applications in plasmas, Elsevier, 2017.

Livadiotis, G.: Kappa distributions: Thermodynamic origin and Generation in space plasmas, 1100, 012 017, <https://doi.org/10.1088/1742-6596/1100/1/012017>, 2018.

Maksimovic, M., Pierrard, V., and Riley, P.: Ulysses electron distributions fitted with Kappa functions, *Geophysical Research Letters*, 24, 1151–1154, <https://doi.org/10.1029/97GL00992>, 1997.

Marsch, E.: Kinetic Physics of the Solar Corona and Solar Wind, *Living Reviews in Solar Physics*, 3, <https://doi.org/10.12942/lrsp-2006-1>, 2006.

Mintzer, D.: Generalized Orthogonal Polynomial Solutions of the Boltzmann Equation, *The Physics of Fluids*, 8, 1076–1090, <https://doi.org/10.1063/1.1761357>, 1965.



Olbert, S.: Summary of Experimental Results from M.I.T. Detector on IMP-1, in: Physics of the Magnetosphere, edited by Carovillano, R. L., McClay, J. F., and Radoski, H. R., pp. 641–659, Springer Netherlands, Dordrecht, ISBN 978-94-010-3467-8, [https://doi.org/10.1007/978-94-010-3467-8\\_23](https://doi.org/10.1007/978-94-010-3467-8_23), 1968.

560 Pierrard, V. and Lazar, M.: Kappa Distributions: Theory and Applications in Space Plasmas, *Solar Physics*, 267, 153–174, <https://doi.org/10.1007/s11207-010-9640-2>, 2010.

Pierrard, V., Maksimovic, M., and Lemaire, J.: Core, Halo and Strahl Electrons in the Solar Wind, *Astrophysics and Space Science*, 277, 195–200, <https://doi.org/10.1023/A:1012218600882>, 2001.

565 Qureshi, M. N. S., Palloccchia, G., Bruno, R., Cattaneo, M. B., Formisano, V., Reme, H., Bosqued, J. M., Dandouras, I., Sauvaud, J. A., Kistler, L. M., Möbius, E., Klecker, B., Carlson, C. W., McFadden, J. P., Parks, G. K., McCarthy, M., Korth, A., Lundin, R., Balogh, A., and Shah, H. A.: Solar Wind Particle Distribution Function Fitted via the Generalized Kappa Distribution Function: Cluster Observations, *AIP Conference Proceedings*, 679, 489–492, <https://doi.org/10.1063/1.1618641>, 2003.

Scherer, K., Fichtner, H., and Lazar, M.: Regularized  $\kappa$ -distributions with non-diverging moments, *Europhysics Letters*, 120, 50002, <https://doi.org/10.1209/0295-5075/120/50002>, 2017.

570 Scherer, K., Lazar, M., Husidic, E., and Fichtner, H.: Moments of the Anisotropic Regularized  $\kappa$ -distributions, *The Astrophysical Journal*, 880, 118, <https://doi.org/10.3847/1538-4357/ab1ea1>, 2019.

Schunk, R. and Nagy, A.: Ionospheres: Physics, Plasma Physics, and Chemistry, Cambridge Atmospheric and Space Science Series, Cambridge University Press, 2009.

575 Schunk, R. W.: Mathematical structure of transport equations for multispecies flows, *Reviews of Geophysics*, 15, 429–445, <https://doi.org/10.1029/RG015i004p00429>, 1977.

Tsallis, C.: Nonadditive entropy Sq and nonextensive statistical mechanics: Applications in geophysics and elsewhere, *Acta Geophysica*, 60, 502–525, <https://doi.org/10.2478/s11600-012-0005-0>, 2012.

Vasyliunas, V. M.: A Survey of Low-Energy Electrons in the Evening Sector of the Magnetosphere with OGO 1 and OGO 3, *Journal of Geophysical Research (1896-1977)*, 73, 2839–2884, <https://doi.org/10.1029/JA073i009p02839>, 1968.

580 Wang, L. and Du, J.: The diffusion of charged particles in the weakly ionized plasma with power-law kappa-distributions, *Physics of Plasmas*, 24, 102 305, <https://doi.org/10.1063/1.4996775>, 2017.